

Diazadimethano[8]circulene: Synthesis, Structure, Properties, and Isolation of Stable Radical Cation

Yusuke Matsuo, Takayuki Tanaka,* and Atsuhiko Osuka

Department of Chemistry, Graduate School of Science, Kyoto University, Sakyo-ku, Kyoto 606-8502, Japan

E-mail: taka@kuchem.kyoto-u.ac.jp

Hetero[8]circulenes have emerged as novel heteroatom-doped polycyclic aromatic hydrocarbons whose properties depend on the constituent aromatic units. Herein we report a C-doped variant, diazadimethano[8]circulene **3**, in which two diphenylcyclopentadiene units are installed into the core of [8]circulene that may prevent effective conjugation. The structure of **3** has been revealed to have two longer C–C bonds in the central eight-membered ring, while the absorption and emission profiles are quite similar to those of tetraaza[8]circulene. Stable radical cation **3⁺** was easily obtained by facile oxidation of **3**. X-ray diffraction analysis of **3⁺** showed a slipped dimer arrangement with negligible intermolecular interaction. Interestingly, the lowest-energy absorption of **3⁺** reaches around 2500 nm, while that of **3** is 447 nm.

Keywords: Hetero[8]circulene | Stable radical cation | S_NAr reaction

Hetero[8]circulene is a class of heteroatom-doped polycyclic aromatic hydrocarbons having a central eight-membered ring.^{1–6} Known repertoires of this class include tetraoxa[8]circulene,² tetrathia[8]circulene,³ tetraselena[8]circulene,⁴ tetraaza[8]circulene,⁵ and their mixed-heteroatom-doped congeners (Figure 1a).⁶ In addition to these, sulfower⁷ and related analogues such as tetrasilatetrathia[8]circulene^{8a} and tetragermatetrathia[8]circulene^{8b} have been reported, thereby expanding the scope of the category. Naturally, increasing attention has been focused on their unique properties and potentials for material

applications such as OLED^{2c} and OFET.⁹ Recently, we have reported that the radical cation of tetrabenzotetraaza[8]circulene **1** is highly stable, allowing its isolation under ambient conditions (Figure 1b).¹⁰ The radical cation **1⁺** exhibited a far red-shifted absorption band reaching 2000 nm. In conjunction with an isolable radical cation of tetraoxa[8]circulene,^{2d} the potential of hetero[8]circulenes to generate their stable radical cations may lead to novel optical and spin materials.

The synthesis of **1⁺** was achieved by S_NAr reaction of diazadithia[8]circulene tetraoxide **2** with aniline derivatives followed by one-electron oxidation with tris(4-bromophenyl)ammonium hexachloroantimonate (Magic Blue).¹¹ It occurred to us that this protocol can be applied for synthesis of other hetero[8]circulene analogues.^{5b} Yorimitsu and co-workers reported an interesting transformation from dibenzothiophene *S,S*-dioxide to a series of spiro-substituted fluorene derivatives by S_NAr reaction.¹² Motivated by this report, we examined the synthesis of diazadimethano[8]circulene **3** in which two diphenylcyclopentadiene units are installed into the core of [8]circulene that may lead to novel properties (Figure 1c). We herein show the synthesis and properties of diazadimethano[8]circulene **3** and isolation and characterization of its radical cation **3⁺**.

Firstly, we prepared *N,N'*-dioctyl-tetrabenzodiazadithia[8]circulene **2** according to the reported procedures.¹⁰ We examined S_NAr reaction of **2** with diphenylmethyl anion that proceeded smoothly in the presence of KHMDS in dioxane, affording tetrabenzodiazadimethano[8]circulene **3** in 68% yield (Scheme 1). High-resolution atmospheric-pressure-chemical-ionization time-of-flight mass-spectrometry (HR-APCI-TOF-MS) revealed the molecular ion peak of **3** at $m/z = 1082.5485$ (calcd for $C_{82}H_{70}N_2 = 1082.5534 [M]^+$). The ¹H NMR spectrum in CD₂Cl₂ showed four peaks due to the benzo-segments at 8.62, 8.04, 7.52, and 7.31 ppm and three peaks due to the phenyl groups in the aromatic region. ¹³C NMR of **3** in CDCl₃ showed a

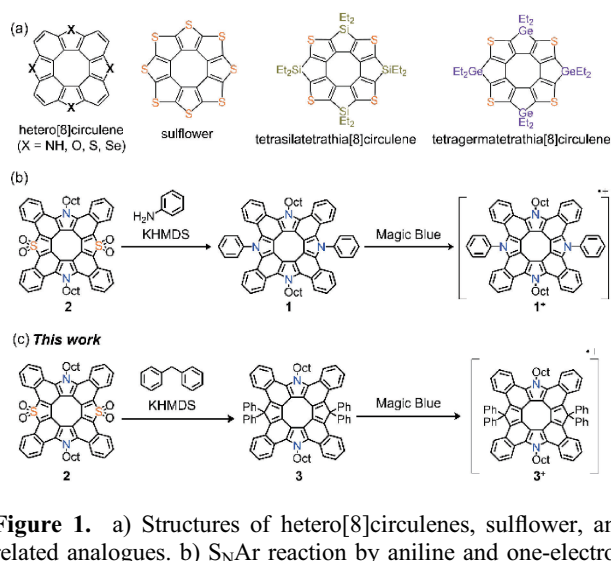
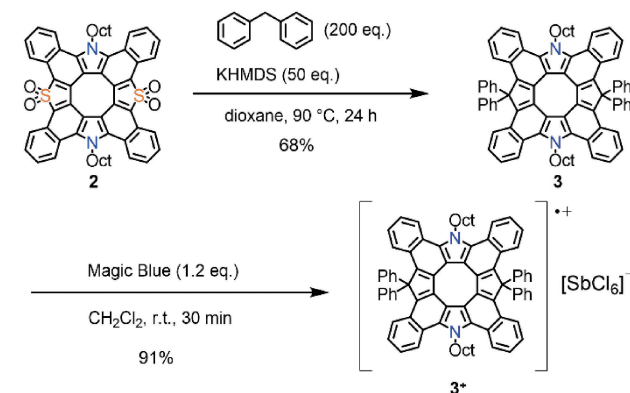


Figure 1. a) Structures of hetero[8]circulenes, sulfower, and related analogues. b) S_NAr reaction by aniline and one-electron oxidation to give tetraaza[8]circulene radical cation **1⁺**. c) S_NAr reaction by diphenylmethane and one-electron oxidation to give diazadimethano[8]circulene radical cation **3⁺** (This work).



Scheme 1. Synthesis of diazadimethano[8]circulene **3** and its radical cation **3⁺**.

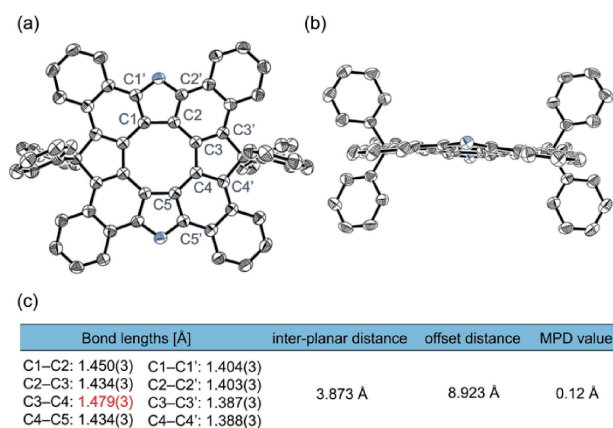


Figure 2. X-ray crystal structures of **3**. a) Top view, b) side view, and c) selected bond-lengths. Thermal ellipsoids are scaled to 50% probability level. Octyl groups and hydrogen atoms are omitted for clarity.

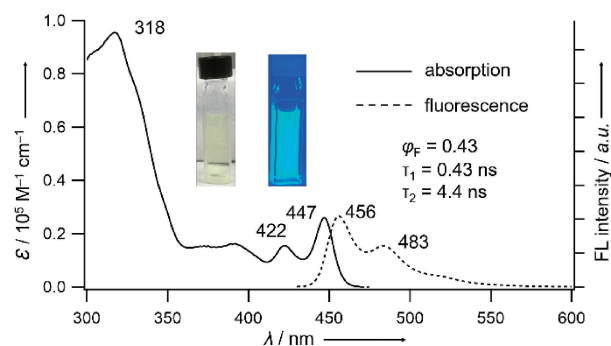


Figure 3. UV/vis absorption (solid) and fluorescence (dashed) spectra of **3** in CH_2Cl_2 (excited at 422 nm).

peak at 65.62 ppm which can be ascribed to the sp^3 -carbon in the core (Figures S1, S2, and S4).

Single crystals of **3** were obtained by slow diffusion of methanol to its dichloromethane solution. A half of the structure has been revealed by X-ray diffraction (XRD) analysis with $P1$ space group.¹³ Among the four C–C bonds constructing the central cyclooctatetraene (COT), the C3–C4 bond is significantly elongated (1.479(3) Å) as compared with others (1.434(3)–1.450(3) Å) (Figure 2). On the other hand, C3–C3' and C4–C4' bonds are slightly shorter (1.387(3) and 1.388(3) Å, respectively), indicating that the contribution of [8]radialene-like conjugation becomes stronger due to the introduction of sp^3 -carbons into the [8]circulene core.^{5a}

Figure 3 shows the UV/vis absorption and fluorescence spectra of **3** in CH_2Cl_2 . A sharp absorption band at 447 nm ($\epsilon = 2.6 \times 10^4 \text{ M}^{-1} \text{ cm}^{-1}$) and its vibronic band at 422 nm were observed. Emission bands were observed at 456 and 483 nm as clear mirror-imaged bands. These peaks are red-shifted as compared with those of **1** probably due to the induction effect by the inserted sp^3 -carbon (Figure S10). The absolute fluorescence quantum yield of **3** was determined to be 43%. The fluorescence lifetime of **3** was measured to be 0.43 and 4.4 ns. The Stokes shift is only 440 cm^{-1} , indicating structural rigidity even in the excited state. These optical properties are similar to those of **1**.

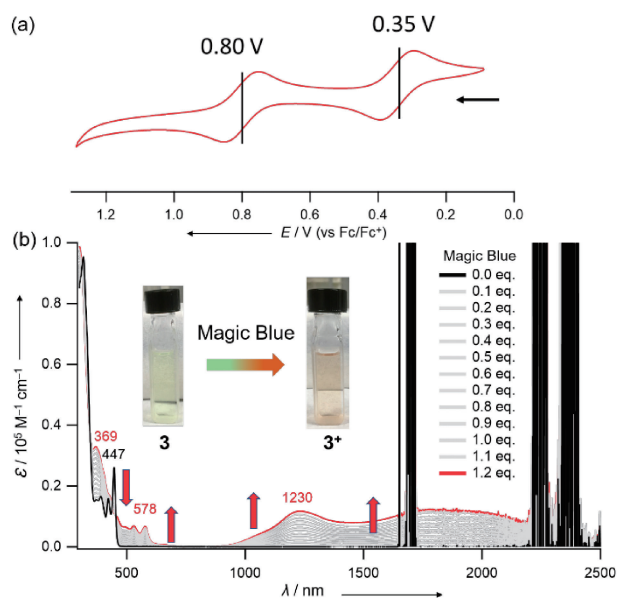


Figure 4. a) Cyclic voltammogram of **3** in CH_2Cl_2 (scan rate: 0.05 V s^{-1} ; working electrode: Pt; reference electrode: Ag/AgNO₃; counter electrode: Pt wire; supporting electrolyte: 0.1 M $n\text{Bu}_4\text{NPF}_6$). b) Absorption spectral changes of **3** in CH_2Cl_2 upon titration with Magic Blue.

Cyclic voltammetry (CV) showed reversible oxidation waves at 0.35 and 0.80 V against Fc/Fc^+ in CH_2Cl_2 (Figure 4a). This suggests that one-electron oxidation is possible by Magic Blue similarly to the case of **1** ($E_{\text{ox},1} = 0.22 \text{ V}$).¹¹ Then, titration of **3** with Magic Blue was conducted to generate the corresponding radical cation, namely $\mathbf{3}^+$. Upon addition of the oxidant, the absorption spectrum of **3** changed with clear isosbestic points at 438 and 454 nm (Figure 4b). Broad NIR bands in the range of 1000–2500 nm were detected which are more red-shifted as compared with $\mathbf{1}^+$. The change was almost saturated upon addition of about 1.2 equivalents of Magic Blue.

The radical cation was isolated in 91% yield after treating **3** with Magic Blue in dry CH_2Cl_2 and purification by silica-gel column chromatography and recrystallization under open air. This radical cation (*i.e.* $\mathbf{3}^+\cdot\text{SbCl}_6^-$, hereafter referred to $\mathbf{3}^+$) is highly stable, and survived in dichloromethane solution even in the presence of MeOH (Figure S14). The structure of $\mathbf{3}^+$ has been revealed by XRD analysis to carry one counter anion (Figure 5a).¹⁴ The MPD value of $\mathbf{3}^+$ is 0.42 \AA , being larger than that of the neutral species **3** (0.12 \AA).¹⁵ The selected C–C bond lengths of the central COT are listed in Figure 5, in which C3–C4 and C7–C8 bonds are still longer (1.462(7) and 1.487(8) Å, respectively). In the packing structure, the closest molecules exist as a slightly stacked dimeric form with an inter-planar distance of 3.460 \AA and an offset distance of 8.855 \AA (Figure 5c). These structural features are different from those of $\mathbf{1}^+$ probably due to the steric repulsion induced by the perpendicularly arranged phenyl groups. The UV/vis/NIR absorption spectrum of isolated $\mathbf{3}^+$ in CH_2Cl_2 was almost identical to that of the titrated spectrum (Figure S11).

The spin-density of $\mathbf{3}^+$ was calculated at the UB3LYP/6-311G(d,p) level without the counter anion using the Gaussian 16 program package.¹⁶ The spin-density is well delocalized over the

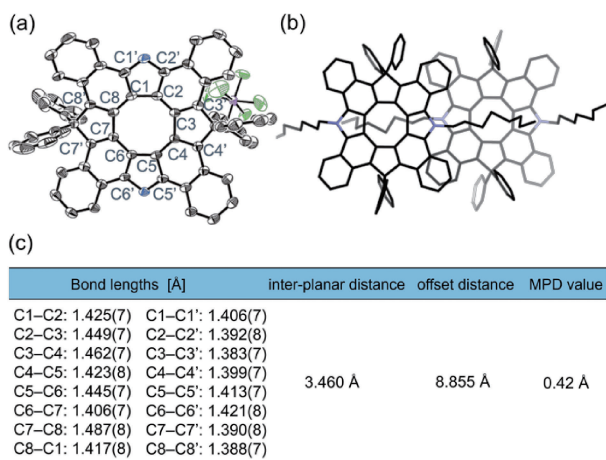


Figure 5. a) X-ray crystal structure of 3^+ . Bond lengths, MPD value, inter-planar distance, and offset distance of 3^+ are shown. Thermal ellipsoids are scaled to 50% probability level. Octyl groups, solvent molecules, and hydrogen atoms are omitted for clarity. b) Packing structure of 3^+ . Counter anions and solvent molecules are omitted for clarity. c) Selected bond lengths.

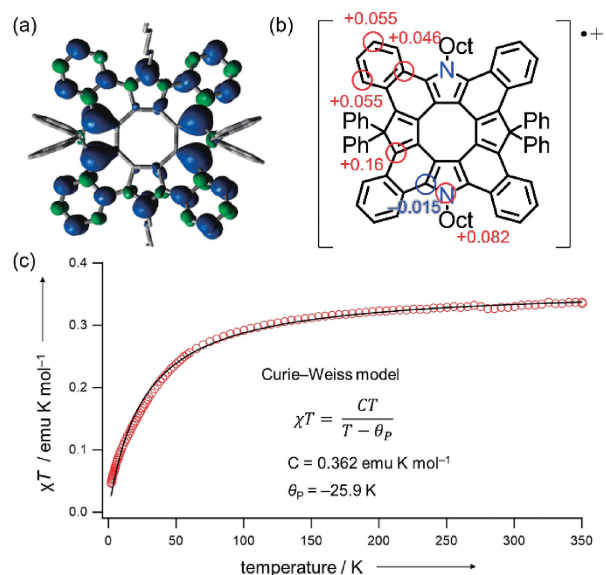


Figure 6. a) Spin-density distribution and b) selected values of 3^+ calculated at the UB3LYP/6-311G(d,p) level (isovalue: 0.001). c) Observed (red circles) and simulated (black line) χT values of 3^+ . Applied field: 0.5 T.

circulene π -system except for the phenyl and octyl groups (Figure 6a). The spin-density is the highest (+0.16) at the cyclopentadiene moiety (C7') while the density at the α -carbon of the *N*-octyl substituted pyrrole (C6') is low (−0.015) (Figure 6b). The ESR spectrum of 3^+ in CH_2Cl_2 /toluene displayed a sharp signal ($g = 2.0040$) at 110 K (Figure S25). The solid-state magnetic properties were investigated by temperature-dependent magnetic susceptibility measurements with SQUID for the polycrystalline sample of 3^+ (Figure 6c). The curve of χT plots were well-reproduced with the Curie–Weiss model with fitting parameters (C , θ_p) = (0.362 emu K mol $^{-1}$,

−25.9 K), where C and θ_p are Curie constant and Curie temperature, respectively. This result indicates that each magnetic moment exists almost independently with rather weak antiferromagnetic intramolecular interactions in the solid state, which is consistent with the crystal packing structure of 3^+ .

The cyclic voltammetry of 3^+ was investigated, which was almost consistent with the results of **3** (Figure S24). The electrochemical gap of 3^+ corresponds to 0.45 eV. In the absorption spectrum of 3^+ , the lowest-energy band reaches 2500 nm. This is somewhat surprising because tetraaza[8]circulene radical cation 1^+ displayed the lowest-energy band up to 2000 nm despite 3^+ possessing less conjugative sp^3 -carbons in the core. TD-DFT calculation for 3^+ well-reproduced the absorption profile, in that the transitions at 1902 nm is mainly attributed to the HOMO(β) \rightarrow LUMO(β) transition (Figure S20). Indeed, the orbital distribution in the frontier molecular orbitals of 3^+ is similar to that of 1^+ , indicating the importance of [8]radialene-like conjugation.^{5a} This tendency has retained even though the C3–C4 and C7–C8 bond lengths are elongated from 1.432(5) and 1.436(2) Å in 1^+ to 1.462(7) and 1.487(8) Å in 3^+ , respectively.

In summary, tetrabenzodiazadimethano[8]circulene **3** that can be regarded as a “C-doped” hetero[8]circulene was synthesized from tetrabenzodiazadithia[8]circulene tetra-oxide **2** via $\text{S}_{\text{N}}\text{Ar}$ reaction with diphenylmethyl anion. Diazadimethano[8]circulene **3** was easily oxidized to give highly stable radical cation 3^+ . The structures of **3** and 3^+ were revealed by X-ray analysis. The calculated spin-density of 3^+ was found to be delocalized over the whole circulene π -system. Interestingly, the absorption and emission spectra of **3** are both red-shifted and the lowest-energy absorption band of 3^+ reaches around 2500 nm. This implies that the optical features of **3** and 3^+ stem from its [8]radialene-like conjugation. Further exploration of the hetero[8]circulenes and hetero[8]circulene variants are actively in progress in our laboratory.

The work was supported by JSPS KAKENHI Grant Numbers (JP18H03910, JP18K14199, and JP20K05463). The authors thank Dr. Ko Furukawa (Niigata Univ.) for ESR measurement and Dr. Kazuya Otsubo (Kyoto Univ.) for PXRD measurement.

Supporting Information is available on <https://doi.org/10.1246/cl.200336>.

References and Notes

- 1 T. Hensel, N. N. Andersen, M. Plesner, M. Pittelkow, *Synlett* **2016**, 27, 498.
- 2 a) H. Erdtman, H.-E. Högberg, *Chem. Commun.* **1968**, 773. b) H. Erdtman, H.-E. Högberg, *Tetrahedron Lett.* **1970**, 11, 3389. c) J. Eskildsen, T. Reenberg, J. B. Christensen, *Eur. J. Org. Chem.* **2000**, 1637. d) R. Rathore, S. H. Abdelwahed, *Tetrahedron Lett.* **2004**, 45, 5267. e) C. B. Nielsen, T. Brock-Nannestad, T. K. Reenberg, P. Hammershøj, J. B. Christensen, J. W. Stouwdam, M. Pittelkow, *Chem.—Eur. J.* **2010**, 16, 13030. f) T. Brock-Nannestad, C. B. Nielsen, M. Schau-Magnussen, P. Hammershøj, T. K. Reenberg, A. B. Petersen, D. Trpceviski, M. Pittelkow, *Eur. J. Org. Chem.* **2011**, 6320.
- 3 a) S. Kato, Y. Serizawa, D. Sakamaki, S. Seki, Y. Miyake, H. Shinokubo, *Chem. Commun.* **2015**, 51, 16944. b) S. Kato, S.

- Akahori, Y. Serizawa, X. Lin, M. Yamauchi, S. Yagai, T. Sakurai, W. Matsuda, S. Seki, H. Shinokubo, Y. Miyake, *J. Org. Chem.* **2020**, *85*, 62.
- 4 X. Xiong, C.-L. Deng, B. F. Minaev, G. V. Baryshnikov, X.-S. Peng, H. N. C. Wong, *Chem.—Asian J.* **2015**, *10*, 969.
- 5 a) F. Chen, Y. S. Hong, S. Shimizu, D. Kim, T. Tanaka, A. Osuka, *Angew. Chem., Int. Ed.* **2015**, *54*, 10639; F. Chen, Y. S. Hong, S. Shimizu, D. Kim, T. Tanaka, A. Osuka, *Angew. Chem.* **2015**, *127*, 10785. b) Y. Nagata, S. Kato, Y. Miyake, H. Shinokubo, *Org. Lett.* **2017**, *19*, 2718. c) F. Chen, Y. S. Hong, D. Kim, T. Tanaka, A. Osuka, *ChemPlusChem* **2017**, *82*, 1048.
- 6 a) C. B. Nielsen, T. Brock-Nannestad, P. Hammershøj, T. K. Reenberg, M. Schau-Magnussen, D. Trpceviski, T. Hensel, R. Salcedo, G. V. Baryshnikov, B. F. Minaev, M. Pittelkow, *Chem.—Eur. J.* **2013**, *19*, 3898. b) T. Hensel, D. Trpceviski, C. Lind, R. Grosjean, P. Hammershøj, C. B. Nielsen, T. Brock-Nannestad, B. E. Nielsen, M. Schau-Magnussen, B. Minaev, G. V. Baryshnikov, M. Pittelkow, *Chem.—Eur. J.* **2013**, *19*, 17097. c) M. Plesner, T. Hensel, B. E. Nielsen, F. S. Kamounah, T. Brock-Nannestad, C. B. Nielsen, C. G. Tortzen, O. Hammerich, M. Pittelkow, *Org. Biomol. Chem.* **2015**, *13*, 5937. d) B. Lousen, S. K. Pedersen, P. Bols, K. H. Hansen, M. R. Pedersen, O. Hammerich, S. Bondarchuk, B. Minaev, G. V. Baryshnikov, H. Ågren, M. Pittelkow, *Chem.—Eur. J.* **2020**, *26*, 4935.
- 7 a) K. Y. Chernichenko, V. V. Sumerin, R. V. Shpanchenko, E. S. Balenkova, V. G. Nenajdenko, *Angew. Chem., Int. Ed.* **2006**, *45*, 7367; K. Y. Chernichenko, V. V. Sumerin, R. V. Shpanchenko, E. S. Balenkova, V. G. Nenajdenko, *Angew. Chem.* **2006**, *118*, 7527. b) L. Li, S. Zhao, B. Li, L. Xu, C. Li, J. Shi, H. Wang, *Org. Lett.* **2018**, *20*, 2181.
- 8 a) Y. Serizawa, S. Akahori, S. Kato, H. Sakai, T. Hasobe, Y. Miyake, H. Shinokubo, *Chem.—Eur. J.* **2017**, *23*, 6948. b) S. Akahori, H. Sakai, T. Hasobe, H. Shinokubo, Y. Miyake, *Org. Lett.* **2018**, *20*, 304.
- 9 a) A. Dadvand, F. Cicoira, K. Y. Chernichenko, E. S. Balenkova, R. M. Osuna, F. Rosei, V. G. Nenajdenko, D. F. Perepichka, *Chem. Commun.* **2008**, 5354. b) T. Fujimoto, R. Suizu, H. Yoshikawa, K. Awaga, *Chem.—Eur. J.* **2008**, *14*, 6053. c) T. Fujimoto, M. M. Matsushita, H. Yoshikawa, K. Awaga, *J. Am. Chem. Soc.* **2008**, *130*, 15790. d) T. Fujimoto, M. M. Matsushita, K. Awaga, *J. Phys. Chem. C* **2012**, *116*, 5240.
- 10 Y. Matsuo, T. Tanaka, A. Osuka, *Chem.—Eur. J.* **2020**, *26*, 8144.
- 11 N. G. Connelly, W. E. Geiger, *Chem. Rev.* **1996**, *96*, 877.
- 12 M. Bhanuchandra, H. Yorimitsu, A. Osuka, *Org. Lett.* **2016**, *18*, 384.
- 13 Crystal data of **3**; Empirical Formula: C₈₂H₇₀N₂; *Mw*: 1083.40; Crystal System: triclinic; Space Group: *P*-1 (No. 2); *a* = 9.4404(19) Å; *b* = 9.7266(14) Å; *c* = 15.7507(13) Å; α = 78.155(14)°; β = 76.302(18)°; γ = 88.61(2)°; *V* = 1374.8(16) Å³; *Z* = 1; density; 1.309 g cm⁻³; completeness: 0.967; goodness-of-fit: 1.035; *R*₁ [*I* > 2σ(*I*): 0.0581; *wR*₂ (all data): 0.1709; CCDC No. 1997256.
- 14 Crystal data of **3**⁺; Empirical Formula: C₈₂H₇₀N₂SbCl₆·2(CH₂Cl₂); *Mw*: 1502.77; Crystal System: monoclinic; Space Group: *P*2/*c* (No. 13); *a* = 18.490(3) Å; *b* = 13.4079(15) Å; *c* = 25.132(4) Å; β = 107.598(6)°; *V* = 6647.9(16) Å³; *Z* = 4; density; 1.502 g cm⁻³; completeness: 0.994; goodness-of-fit: 1.312; *R*₁ [*I* > 2σ(*I*): 0.0960; *wR*₂ (all data): 0.3189; CCDC No. 1997257.
- 15 The MPD values were defined by the 44 core atoms consisting of four benzene, two pyrrole, and two cyclopentadiene units.
- 16 Gaussian 16, Revision A.03, M. J. Frisch, G. W. Trucks, H. B. Schlegel, G. E. Scuseria, M. A. Robb, J. R. Cheeseman, G. Scalmani, V. Barone, G. A. Petersson, H. Nakatsuji, X. Li, M. Caricato, A. V. Marenich, J. Bloino, B. G. Janesko, R. Gomperts, B. Mennucci, H. P. Hratchian, J. V. Ortiz, A. F. Izmaylov, J. L. Sonnenberg, D. Williams-Young, F. Ding, F. Lipparini, F. Egidi, J. Goings, B. Peng, A. Petrone, T. Henderson, D. Ranasinghe, V. G. Zakrzewski, J. Gao, N. Rega, G. Zheng, W. Liang, M. Hada, M. Ehara, K. Toyota, R. Fukuda, J. Hasegawa, M. Ishida, T. Nakajima, Y. Honda, O. Kitao, H. Nakai, T. Vreven, K. Throssell, J. A. Montgomery, Jr., J. E. Peralta, F. Ogliaro, M. J. Bearpark, J. J. Heyd, E. N. Brothers, K. N. Kudin, V. N. Staroverov, T. A. Keith, R. Kobayashi, J. Normand, K. Raghavachari, A. P. Rendell, J. C. Burant, S. S. Iyengar, J. Tomasi, M. Cossi, J. M. Millam, M. Klene, C. Adamo, R. Cammi, J. W. Ochterski, R. L. Martin, K. Morokuma, O. Farkas, J. B. Foresman, D. J. Fox, Gaussian, Inc., Wallingford CT, **2016**.